Journal of
Applied Sciences

Performance Assessment of Ventilated BIPV Roofs Collocating With Outdoor and Indoor Openings

[1]I-Jyh Wen, [1]Pei-Chi Chang, [2]Che-Ming Chiang and [3]Chi-Ming Lai
[1]School of Engineering Science and Technology,
National Yunlin University of Science and Technology, Taiwan
[2]Department of Architecture, National Cheng-Kung University, Taiwan
[3]Department of Civil Engineering, National Cheng-Kung University, Taiwan

Abstract: In this study, ventilated BIPV (Building Integrated Photovoltaic) has been designed and developed with a double skin roof structure to introduce indoor ventilation and provide itself with environmental control. The influence of BIPV opening locations (toward the outdoor and indoor) with different wind velocities on PV heat dissipation, air exchange rates and average indoor temperature are analyzed, via CFD numerical simulations. It shows that, in different wind conditions, ventilated BIPV roofs with outdoor and indoor openings have different capabilities in air exchange and thermal environment. Both designs proposed in this study can achieve adequate indoor thermal environments and maintain PV panel temperatures within an acceptable range.

Key words: BIPV (building integrated photovoltaic), ventilation, CFD (computational fluid dynamics), double roof

INTRODUCTION

A deficiency of energy is currently the greatest threat to society on a global scale. Energy saving, directly from building design, can make a significant contribution to the sustainable development of people. BIPV (Building Integrated Photovoltaic) plays an important part in current sustainable building design. With the advantages of reduction in overall construction cost and increase of PV (Photovoltaic) installation quantity, BIPV is worthy of development. However, there is a significant issue when using BIPV: under direct sunshine, temperature of PV panels increase and reduce the power generation from PV. An appropriate solution is to design a BIPV structure which can remove its own heat gain and induce ventilation naturally from rooms simultaneously.

In this study, ventilated BIPV has been designed and developed with a double skin roof structure to provide BIPV with environmental control and indoor ventilation induction. The influence of BIPV opening locations (toward the outdoor and indoor) with different outdoor wind velocities on PV heat dissipation, indoor air exchange rates and average temperature are analyzed. The findings will serve as reference for design of new buildings, renovation of existing buildings and future studies.

Development from PV to BIPV: As the installation of PV and BIPV increase significantly, buildings with PV skin will become a synonym for ecological buildings, innovation and technology (Benemann *et al.*, 2001). To achieve BIPV, PV is integrated into the building skin, making the system, in addition to power generation, become a structural part of the building. It can further replace the current building skin materials to reduce cost. Working with sunshades and illumination design, BIPV can increase the energy saving of buildings. BIPV transforms buildings from passive energy consumers to active power generators. This is an important step toward sustainable development.

BIPV has several advantages:

- Power generation and use at the original site to reduce expenses and energy consumption on power line
- Saving space on placement of PV panels and their support structures
- New types of building materials can be applied to save expensive exterior decoration materials (e.g., glass walls) and reduce the cost of the buildings, making the appearance of the buildings more appealing

- During peak load period, BIPV, in addition to guaranteeing electricity demand inside the buildings, can also supply power to utility lines
- BIPV eliminates air pollution from regular fossil fuel power generation, which on a large scale can significantly affect the quality of life
- PV panels, which were placed on (or integrated with) roofs or walls, can reduce the cooling load of air conditioners and produce an adequate indoor thermal environment

PV panels can be integrated into the building facade and replaced glass walls, arch glass (transparent or semiopaque part) or wall materials (opaque part); integrated into the semiopaque skylights; integrated into the external sunshades on windows or replaced the other outer skin of buildings. Common installation of BIPV are in the roof, atrium glass top, skylight or glass houses (green houses), vertical sides of houses and sunshades (DSG, 2005).

Influence of solar heat gain on BIPV: Please refer to (Roger and Ventre, 2000) for influences of temperature rise on PV. The power generation provided by suppliers of crystal silicon PV is under standardized testing conditions (AM1.5, 25°C, 1000 W m^{-2}). In normal use, it is very difficult to maintain 25°C of PV (or plate bottom of the PV module). When the temperature exceeds 25°C, the performance of cells reduces, affecting the power generation of the PV system. In other words, the solar radiation, other than that converted into power by PV, is transferred into heat, increasing the temperature of PV and the surrounding temperature which affects power generation performance.

When designing PV systems, in addition to strength of solar radiation, it is also necessary to consider the requirements of ventilation on the back of PV. The requirements are related to effective dispersion of PV due to increased temperature. PV systems directly exposed to sunshine will naturally increase in temperature. According to data, PV temperature must be maintained below 70°C. From experience in Europe (Prasad and Snow, 2005), systems on the facade of houses without reserved air space, will have 10% loss of BIPV performance of electricity generation. With 5 cm reserved space, the loss is 5%. With 15 cm space, the loss will be negligible.

Solutions to heat impact: Ventilated BIPV: Temperature is the most significant factor affecting the power generation performance of PV. The best solution to reduced power generation of PV due to increased temperature of PV in BIPV due to sunshine is to design the BIPV structure with environmental control to take away the heat gain of BIPV naturally. As above there is an absolute relationship between ventilation and PV in BIPV. The following paragraphs will further discuss literature and the effect of ventilated BIPV on reduction of cooling load of air conditioners.

Yang *et al.* (2000) analyzed ventilated BIPV via simplified analytic method. The system was designed integrating PV and brick walls. The width and height of BIPV is 1.06 and 3.564 m where the brick wall was 24 cm thick. Room temperature was set 20°C and air flow channel width 12 cm to evaluate the reduction of cooling load by ventilated BIPV with ξ (cooling load component reduction ratio). ξ is defined in Eq. 1:

$$\xi = \frac{S_w - S_{pv}}{S_w} \qquad (1)$$

Where:
S_w : The required cooling load of brick walled body
S_{pv} : The required cooling load of BIPV wall body

Findings show that, in the Hong Kong climate, the load reduction ratio of ventilated BIPV was 32.5%. Those in Shanghai and Beijing were 41.1 and 50.1%, respectively. Yun *et al.* (2007) included power generation performance, energy saving of illumination from daylight, room ventilation and energy savings from building skin coverage with ventilated BIPV into consideration and propose a comprehensive evaluation indicator--PVEF (Effectiveness of a PV Facade) as in Eq. 2. The analysis includes the climatic conditions where buildings are located, room depth (distance to windows) and illumination load. The findings show that, with an increase of BIPV light transmittance, cooling load of air conditioners and illumination energy savings immediately improve; while power generation and heating load were reduced. PVEF provides the optimum at 30% light transmittance:

$$PVEF = \frac{L_{saving} + E_{output}}{H_{energy} + C_{energy}} \qquad (2)$$

Where:
L_{saving} : Illumination energy saving from introduction of daylight
E_{output} : Power generation from PV
H_{energy} : Heating load
C_{energy} : Cooling load

Current research on the reduction of cooling load for ventilated BIPV do not incorporate similar BIPV

constructions to be adequately compared with this study. As such, materials which can be cited are limited. It appears ventilated BIPV tends to easily have capability of self environment control. Its design would induce indoor ventilation via thermal buoyancy and wind power, which reduces indoor cooling load as well as increases thermal insulation performance.

Ventilated BIPV developed from double skin structure:
Double skin is used to develop ventilated BIPV enabling BIPV to induce Indoor ventilation and reduce the cooling load potentially. Double-skin structure enables the mezzanine to form an air layer. In summer, the air layer with opened ends can reduce the heat entering into the room; in winter, the air layer with closed ends can reduce the heat loss from inner building to outer cold environment (Chang *et al.*, 2008). When an open-ended parallel-plate channel (formed in the double roof design) exposed to solar irradiation, a part of irradiation (source heat) will be reflected from the outer surface of upper plate. Since the surface is opaque, the rest of irradiation will be absorbed and heat the plate. With a higher temperature, the upper plate will then dissipate its heat to both outside environment (via radiation and convection) and inner channel (via radiation and convection). By receiving the radiation from the upper plate, the temperature of lower plate will also be heated up. It's energy will in turn dissipate either to inner air, or further downward. The air inside the channel, which is practically radiation transparent, will be heated up after absorbing the convection heat from both upper plate and lower plate. Due to the buoyancy effect, the heated air will flow upward and exit out of the upper right end while the make-up colder air will continuously flow into the channel via the lower left end (Lai *et al.*, 2008).

Brinkworth *et al.* (1997) uses numerical analysis to explore the ventilation effects of ventilated BIPV in PV and stone walls, with an air flow channel width of 12 and 24 cm thick stone wall. Outdoor sunshine was measured at 620 W m^{-2} with $15 \sim 22°C$ outdoor air temperature and $1.8 \sim 3.2$ m sec^{-1} wind velocity. Color of PV back panel and surface of stone wall (both sides of the flow channel) were black (both absorption and emittance are 0.9) to predict the relationship between ventilation rates and height of BIPV. Brinkworth *et al.* (1997) use a unit space of W (m) in length (also the length of PV panels), Y (m) in width and 3 (m) in height with average air flow channel speed at 0.25 m sec^{-1}. The ventilated BIPV can induce indoor ventilation at around 36/Y (in ACH). The findings show that, when space width Y is 6 m, the induced indoor ventilation from ventilated BIPV was 6 ACH. A higher Y value will lead to reduced indoor ventilation.

In future, designs of BIPV, it will be necessary to use advanced methods of ventilation. Attention must be given to room space and ventilation paths to fully develop the performance of ventilation of ventilated BIPV.

RESEARCH METHOD

Investigated model classroom: According to the research on house and school modules by the Building Research Institution, Ministry of the Interior, Taiwan, most elementary school classrooms of lengths of 9 m and widths of 7.2-7.8 m are commonly constructed of reinforced concrete. This study investigated a classroom with the size of 9×7.5 m. According to the domestic Building Codes regarding classroom space, the height of the overhang is about 3 m, as depicted schematically in Fig. 1. According to a survey on the window designs of elementary school classrooms, the size of each window is
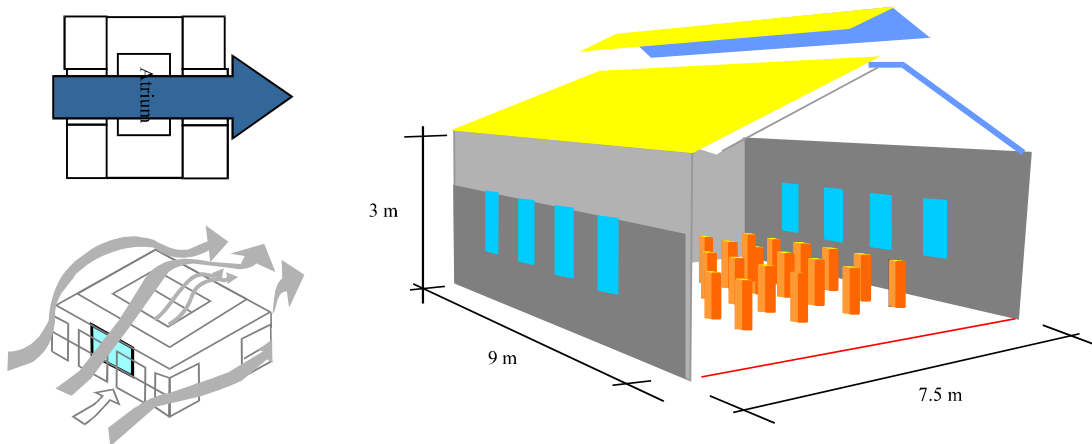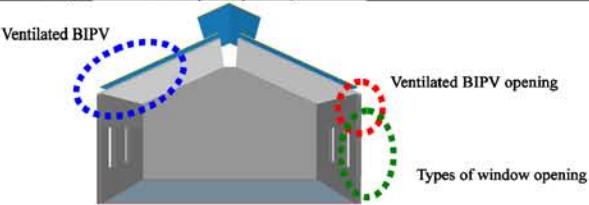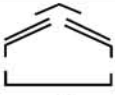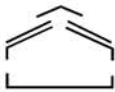

Fig. 1: Diagram of classroom on the upper floor commonly seen in Taiwan

Table 1: Dimensional parameters specified in numerical calculation

Parameters	Condition	
	Air velocity	Wind velocity: 0.1 and 2 m sec^{-1}
Outdoor environment	Outdoor temperature	Atmospheric temperature (Summer, 29°C)
	Solar heat gain at the PV panel	Max. daily solar radiation (1020 W m^{-2})
Construction	Roof	Ventilated BIPV roof (upper plate: PV; lower plate: reinforced concrete)
		CRSO (wave-shaped steel plate)
		Slope of the roof (23.5°)
		Air layer thickness within double roof (10 cm)
	Overhang opening	Overhang opening area (10×450 cm)
		Controlled variables: Overhang opening toward outside or indoor
	Ridge opening	Ridge opening area (50×450 cm)
	Wall opening	The location and opened area of windows in the 2 design mix are the same
		Area of the crack between the door and its frame (3×100 cm)
Indoor	Lighting equipment	Heat dissipation of the lighting equipment is out of consideration
	Thermal resource	Thermal resource of students is out of consideration

Table 2: Configurations for numerical simulation (no means not open/operate)

Mode	Ventilated BIPV	BIPV opening	Types of window	Illustrative
Outdoor mode	Yes	Outdoor	Yes (parallel)	
Indoor mode	Yes	Indoor	Yes (parallel)	

commonly 1.2 m (height)×1.2 m (width), which can provide a ventilation opening of 1.2 m (height)×0.6 m (width). In the discussion meeting of the program Sustainable Construction for Renovated and New School Buildings, held by the Ministry of Education in 1994, there stipulated ten regulations. One regulation is: taking how to make a better indoor air environment? into consideration in the design process and utilizing natural ventilation approach is then high recommended. The windows have the same total opened area with conventional windows and are identically 1.2 m (height)×0.6 m (width). Numerical simulations have been undertaken for the steady-state, three dimensional turbulent flow in 2 natural ventilation design mix (double roof, CRSO (Covered Ridge with Sidewall Opening) and windows), with the following parameter configurations shown in Table 1. The other dimensional parameters specified in this study are shown in Fig. 2.

Physical problems: CFD (Computational Fluid Dynamics) simulations were carried out to investigate how the two natural ventilation design mix (double roof, CRSO (Covered Ridge with Sidewall Opening), roof ridge

opening, windows and BIPV opening location) influence indoor thermal environment during the summer season with outdoor wind velocity. The contents of the mixes are shown in Table 2. Every condition is the same, except the controlled variables marked in Table 1: (1) whether it has a double roof; (2) where the BIPV opening is located; (3) types of windows. Furthermore, the thermo-physical properties of the air are independent of temperature, except for the density, for which the Boussinesq approximation is valid.

Numerical method: Numerical simulations of the physical problem under consideration have been performed via a finite volume method for solving the governing equations and boundary conditions described earlier. A commercial CFD code, PHOENICS, was used to simulate the airflow and temperature distributions. The governing equations solved by PHOENICS include the three-dimensional time-dependent incompressible Navier-Stokes equation, time dependent convection diffusion equation and k-ε turbulence equations. These formulated equations can be found in the PHOENICS user's manual (Spalding, 1994) as well as any CFD textbook and will not be provided here.

Due to its symmetry of the physical problem, the geometric figure under investigation can be (900×750)/2 and contains 15 students

200

500

200

750

CRSO (Covered Ridge with Sidewall Opening)

100

50

200

Ventilated BIPV

PV pannel

RC

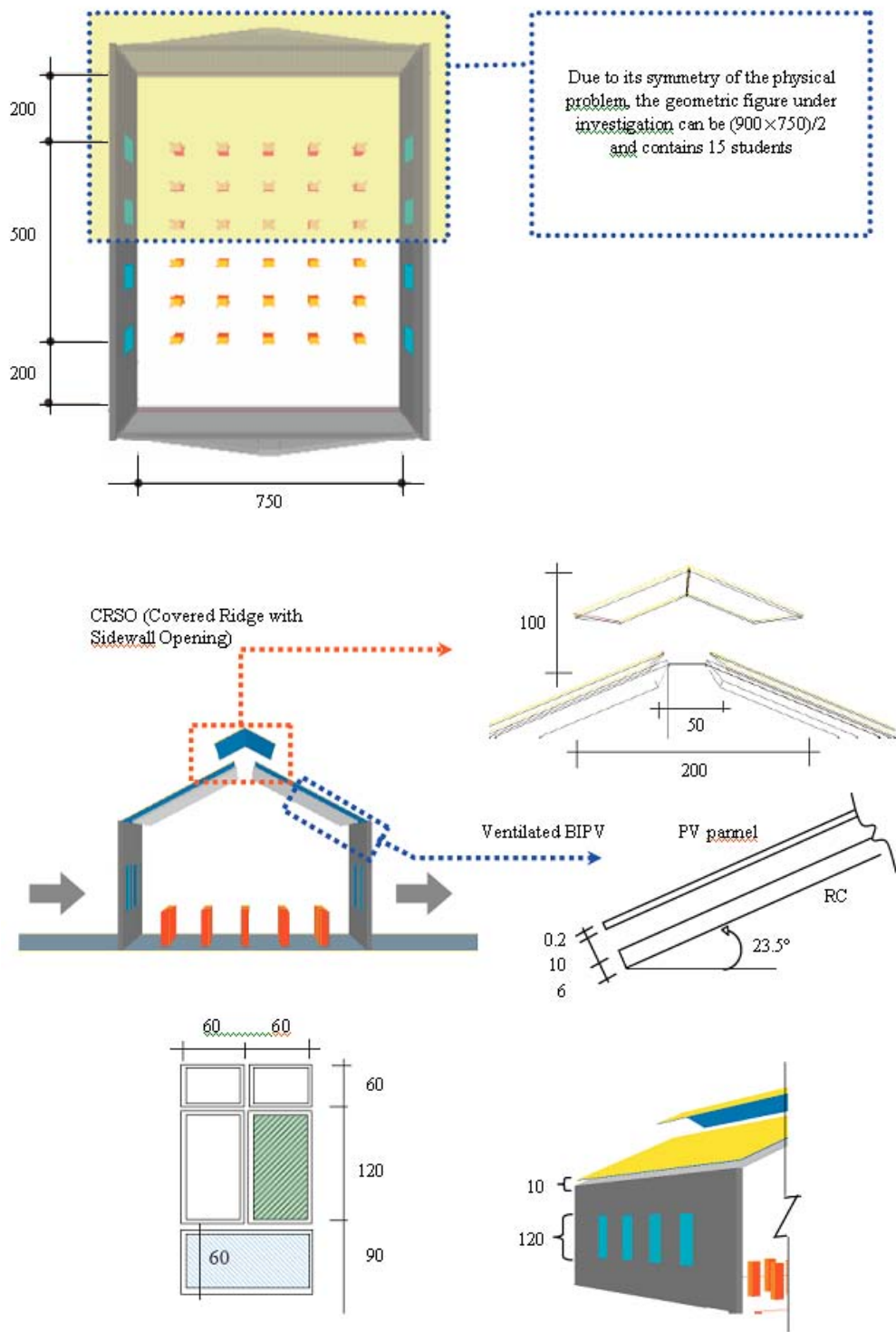0.2
10
6

23.5°

60   60

60

120

90

60

10

120

Fig. 2: Schematic diagram of the investigated classroom (cm)

For the k-ε turbulence equation, the empirical turbulence coefficients were assigned as: $\sigma_k = 1.0$, $\sigma_c = 1.22$, $\sigma_{c1} = 1.44$, $\sigma_{c2} = 1.92$ and $C\mu = 0.09$, respectively. These values were widely accepted in CFD k-ε model. To bridge the steep dependent variable gradients close to the solid surface, the general wall function is employed. The iteration calculation was continued until a prescribed relative convergence of 10^{-3} is satisfied for all field variables of this problem. Numerical simulation accuracy depends on the resolution of the computational mesh and a finer grid leads to solutions that are more accurate. In this study, a grid system with approximately 133×36×97 cells was used for numerical simulation. The increase of cell number will provide information that is more favorable; however, it will be accompanied by a significant increase of computation resources.

RESULTS AND DISCUSSION

Numerical simulation results of outdoor mode
Description of flow structure: Figure 3 shows the flow structure of outdoor wind going through Outdoor Mode at a velocity of 0.1 m sec^{-1} (calm wind). When the outdoor wind flows over a ventilated BIPV roof, the net flow area between free stream and roof panel becomes smaller. The wind velocity increase at the entrance of the CRSO and is measured at a speed of 1 m sec^{-1}. In the CRSO, airflow from A1 induces the room airflow A2 outdoors, flowing to the right of the CRSO; at the same time of flowing out from CRSO, the two air streams form A4 airflow due to the shape of the CRSO and the influence of A3 buoyant airflow above the right roof panel.

When outdoor wind velocity increases to 2 m sec^{-1} (slight breeze), the main flow structure is similar to that of the 0.1 m sec^{-1} case as in Fig. 4. However, the detailed flow structure close to the CRSO is greatly different from the previous case. The outdoor air flows through the CRSO at a higher speed (around 3.75 m sec^{-1}) and induces indoor airflow A2 to CRSO. The air stream from the two sides of A2 will return indoors after touching the roof, failing to flow outdoors with A1. The two returned airflows A2R and A2L form, respectively 2 air circulations, affecting heat dissipation on the roof panels.

Indoor air movement: As in Fig. 5, the outdoor air at a wind velocity of 0.1 m sec^{-1} flows indoor from the left windows (B1 stream). Part of the B1 stream, affected by thermal buoyancy near the roof panel and airflows through CRSO, is attracted to move upwards to form the B2 stream, which has a small flow velocity but smoothly flows through beneath the left roof and takes away the solar heat gain at the roof. Most of the B1 stream penetrates indoors and flows outdoors from the right windows. Some airflows touch the upper wall of the right side window, forming the B3 stream, which flows through beneath of the right side roof and takes the heat above the roof away to flow backwards to the CRSO. Then it is combined with the B2 stream and flows outdoors at a velocity of around 0.28 m sec^{-1} through the CRSO.

When outdoor wind velocity reaches 2 m sec^{-1}, the indoor flow structure is basically similar to the previous case at 0.1 m sec^{-1}. The detailed flow structure differs greatly as in Fig. 6. Compared with the previous case, the indoor B1 stream is attracted by the A2 stream at a higher
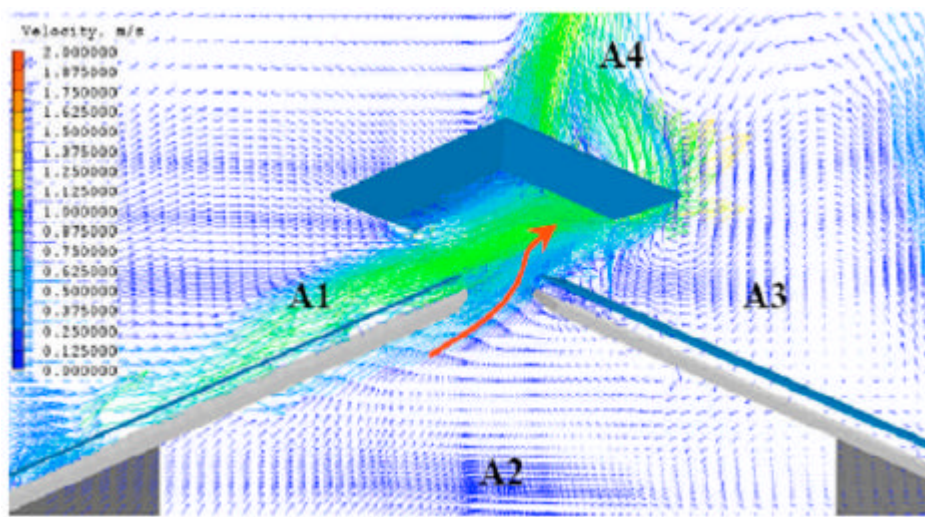

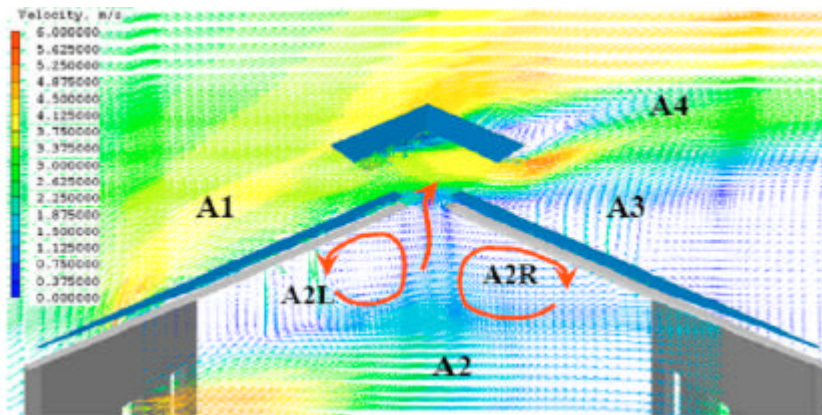Fig. 3: Flow structure around the ventilated BIPV at the outdoor mode with 0.1 m sec^{-1} wind velocity

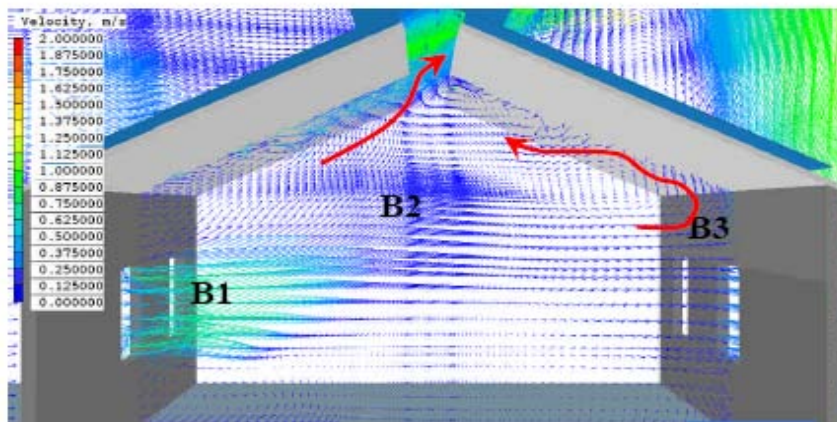Fig. 4: Flow structure around the ventilated BIPV at the outdoor mode with 2 m sec^{-1} wind velocity

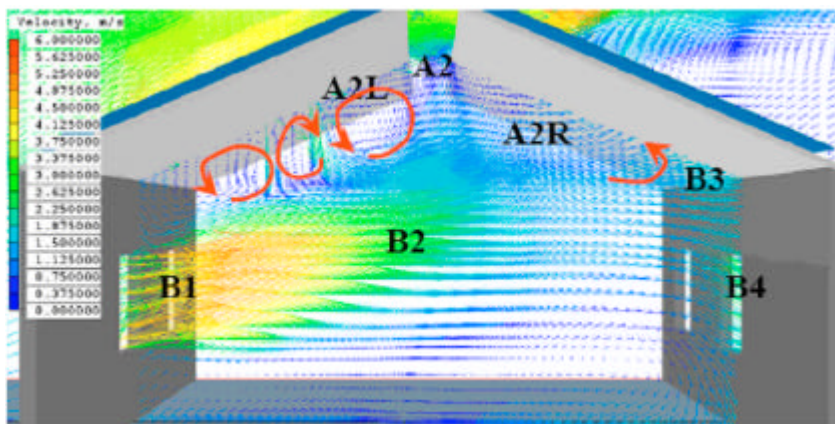Fig. 5: Indoor flow structure at the outdoor mode with 0.1 m sec^{-1} wind velocity

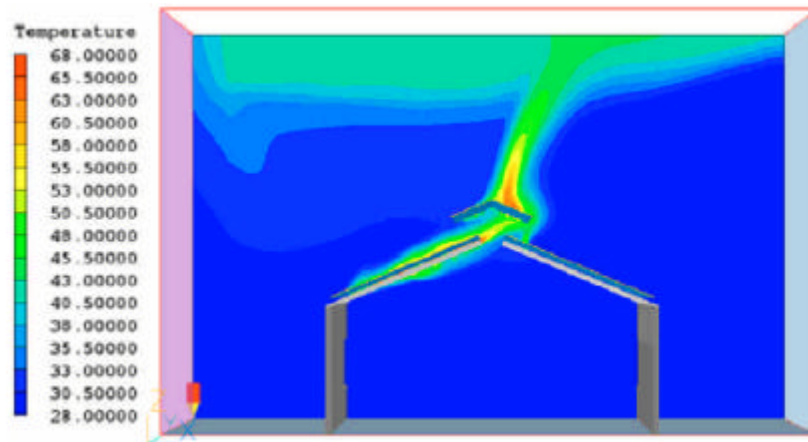Fig. 6: Indoor flow structure at the outdoor mode with 2 m sec^{-1} wind velocity

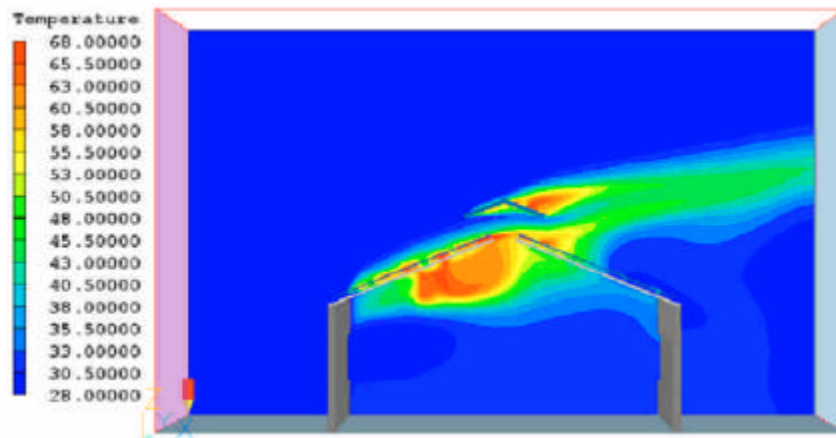Fig. 7: Temperature distribution at the outdoor mode with 0.1 m sec⁻¹ wind velocity

Fig. 8: Temperature distribution at the outdoor mode with 2 m sec⁻¹ wind velocity

flow velocity, resulting in more airflow movement to the CRSO, forming a B2 stream. Affected by B2 stream, A2L stream and roof, the air below the roof panel will form multiple secondary circulations, making it difficult to dissipate solar heat gain at the roof panel. The B3 stream on the right will encounter A2R, causing all airflows to stagnate. Heat of the roof is not easily removed.

Indoor temperature distribution: As in Fig. 7, when the outdoor wind velocity is 0.1 m sec⁻¹, even with an air current flowing above the roof, the double skin roof still fails to effectively take away the heat gain. The temperature of the roof on the left rises. However, indoor air flows smoothly and takes the top left air current to the ridge so that heat gain does not stay in the house. Temperature in the house does not significantly rise. In the simulation result, the average room temperature is 29.58°C. Under 3 m in the room was measured at 29.02°C, with a room ceiling temperature around 32.18°C.

When the outdoor wind velocity reaches 2 m sec⁻¹, affected by the preceding flow structure, circulation below the roof will cause heat to accumulate at the room ceiling, as shown in Fig. 8. In the simulation result, the average room temperature was 37°C. The room under 3 m was 34.13°C. Room ceiling temperature was as high as 50.97°C.

Numerical simulation results of indoor mode: The indoor mode had openings for a double roof structure in the room. Therefore, the major flow structure was similar to that of the outdoor mode. What was different was in the indoor mode, the air in the channel of the double roof flowed from the low opening to the CRSO as C1 and C2 in Fig. 9, unlike that in the previous case of the outdoor mode. At outdoor mode, outdoor air currents flowed into the channel, blocking the flow of buoyant flow in the channel. As a result, the double roof design of indoor mode had greater performance and effectively took away the heat on the roof.
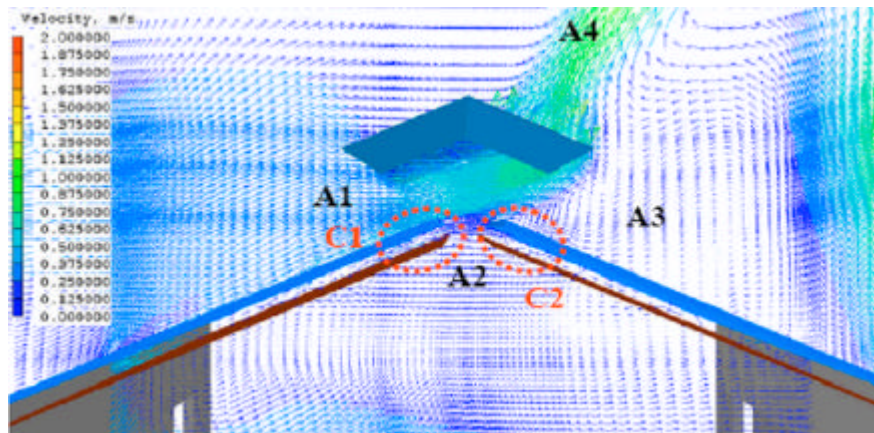
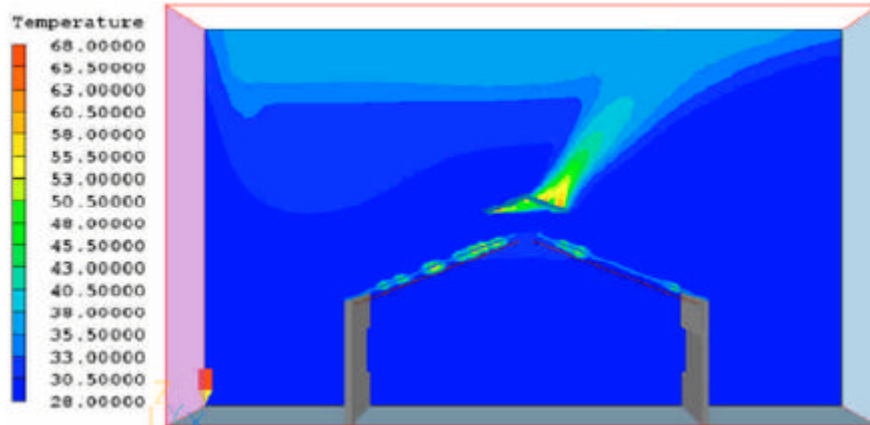Fig. 9: Flow structure around the ventilated BIPV at the indoor mode with 0.1 m sec⁻¹ wind velocity

Fig. 10: Temperature distribution at the basic mode with 0.1 m sec⁻¹ wind velocity

When outdoor wind velocity was 0.1 m sec⁻¹ (Fig. 10), the average room temperature was 29.4°C; under 3 meters was 29.14°C and at the ceiling 30.63°C. As outdoor wind velocity reached 2 m sec⁻¹ (Fig. 11), the average room temperature was 29.19, 29.07°C under 3 m with a ceiling temperature of 29.81°C.

Comparisons of the two modes
Air exchange rates: Under wind velocity of 0.1 m sec⁻¹, the air exchange rates of outdoor and indoor mode are 31 (ACH) and 27 (ACH), respectively. Outdoor mode is larger than that of indoor mode by 1.15 times. This shows that, under calm conditions, the outdoor mode with an outward opening has better ventilation than the Indoor mode with inward openings. Under wind velocity of 2 m sec⁻¹, the air exchange rates of outdoor and indoor mode are 123 (ACH) and 141 (ACH), respectively. Indoor mode is larger than that of the outdoor mode. The outdoor mode was 0.87 times the indoor mode. The main reason is, when outdoor

wind flows more quickly, the indoor air current of the outdoor mode, limited by the flow structure near the CRSO, fails to release from the ridge opening, resulting in the indoor mode have better natural ventilation performance.

Average indoor temperature: Under wind velocity of 0.1 m sec⁻¹, the average temperature of outdoor and indoor mode are 29.58 and 29.4°C, respectively. Outdoor mode is 0.18°C, or 0.6% higher than that of indoor mode. In calm wind conditions, the room temperature distributions of the two modes do not differ significantly. Under wind velocity of 2 m sec⁻¹, the difference is distinctive. The outdoor mode was 7.8°C, or 27% higher than that of indoor mode. This proves that when external environment has stronger wind, a double skin roof with openings to the indoor has a more adequate thermal environment.
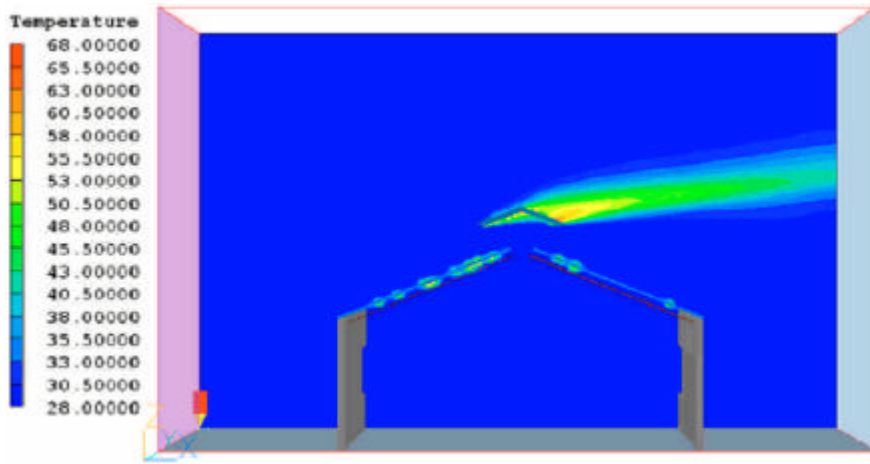
Fig. 11: Temperature distribution at the indoor mode with 2 m sec^{-1} wind velocity

Fig. 12: Comprehensive evaluation of outdoor mode and indoor mode

Comprehensive evaluation: Figure 12 shows the influences of outdoor mode (with outdoor openings with opened windows of BIPV) and indoor mode (indoor openings with opened windows with a double skin BIPV roof) on natural ventilation and thermal environment, via air exchange rates and average temperature.

CONCLUSION

Air exchange with natural ventilation: In calm wind conditions (0.1 m sec^{-1} outdoor wind), the natural ventilation effect of outdoor opening double skin BIPV has better performance than double skin BIPV with indoor openings; in a light wind state (2 m sec^{-1} outdoor wind), the result is opposite.

Thermal environment comfort: In both calm and light wind states, the level of the thermal environment comfort using double skin BIPV with indoor openings show better performance than double skin BIPV with outdoor openings. In a calm wind state, the average room temperature of the two is around 29°C. In a light wind state, however, the average room temperature of double

skin BIPV with indoor openings still remains at around 29°C while the double skin BIPV with outdoor openings is as high as 37°C.

PV panel temperature: In both calm and light wind states, temperatures of PV bottom panel of both Modes are around 55~68°C. It shows that both ventilated BIPV designs proposed in this study can achieve adequate indoor thermal environments and control PV panel temperatures within an acceptable range.

REFERENCES

Benemann, J., O. Chehab and E. Schaar-Gabriel, 2001. Building-integrated PV modules. Solar Energy Mater. Solar Cells, 67: 345-354.

Brinkworth, B.J., B.M. Cross, R.H. Marshall and H. Yang, 1997. Thermal regulation of photovoltaic cladding. Solar Energy, 61: 169-178.

Chang, P.C., C.M. Chiang and C.M. Lai, 2008. Development and preliminary evaluation of double roof prototypes incorporating RBS (Radiant Barrier System). Energy Build., 40: 140-147.

DSG, 2005. Planning and Installing Photovoltaic Systems. 2nd Edn. James and James Ltd., London, UK., ISBN: 9781844074426. .

Lai, C.M., J.Y. Huang and J.S. Chiou, 2008. Optimal spacing for double-skin roofs. Build. Environ., 43: 1749-1754.

Prasad, D. and M. Snow, 2005. Designing with Solar Power: A Source Book for Building Integrated Photovoltaic. New Edn. The Images Publishing Group Pvt. Ltd. and Earthscan, London, UK., ISBN: 1844071472, pp: 50-52.

Roger, M. and J. Ventre, 2000. Photovoltaic Systems Engineering. 2nd Edn. The CRC Press, Boca Raton Florida, USA., ISBN: 9780849317934, pp: 45-46.

Spalding, D.B., 1994. The PHOENICS Encyclopedia. 2nd Edn. CHAM Ltd., London, UK .

Yang, H., J. Burnett and J. Ji, 2000. Simple approach to cooling load component calculation through PV walls. Energy Build., 31: 285-290.

Yun, G.Y., M. McEvoy and K. Steemers, 2007. Design and overall energy performance of a ventilated photovoltaic façade. Solar Energy, 81: 383-394.